NASA TECHNICAL NOTE

NASA TN D-5394

SIMPLIFIED ANALYTICAL MODEL FOR USE IN DESIGN OF PUMP-INLET ACCUMULATORS FOR THE PREVENTION OF LIQUID-ROCKET LONGITUDINAL OSCILLATION (POGO)

by William Lewis

Lewis Research Center
Cleveland, Ohio

NATIONAL AERONAUTICS AND SPACE ADMINISTRATION • WASHINGTON, D. C. • AUGUST 1969

SIMPLIFIED ANALYTICAL MODEL FOR USE IN DESIGN OF PUMP-INLET ACCUMULATORS FOR THE PREVENTION OF LIQUID-ROCKET LONGITUDINAL OSCILLATION (POGO)

By William Lewis

Lewis Research Center
Cleveland, Ohio

NATIONAL AERONAUTICS AND SPACE ADMINISTRATION

For sale by the Clearinghouse for Federal Scientific and Technical Information
Springfield, Virginia 22151 – CFSTI price $3.00

ABSTRACT

Prevention of pogo by means of an accumulator at the pump inlet is facilitated by a simplified analytical model that expresses the net in-phase force feedback in terms of the admittance of the accumulator, thereby providing a frame of reference for the use of judgment in the design. Treating the effects of the fuel and oxidizer systems as independent and additive and reckoning force feedback at the structure modal frequency only permit a simple description of the primary mechanism. A novel feature of the model is that the effect of outflow perturbations on tank-bottom pressure is included in the net-thrust function.

SIMPLIFIED ANALYTICAL MODEL FOR USE IN DESIGN OF PUMP-INLET ACCUMULATORS FOR THE PREVENTION OF LIQUID-ROCKET LONGITUDINAL OSCILLATION (POGO)

by William Lewis

Lewis Research Center

SUMMARY

Prevention of pogo by means of an accumulator at the pump inlet is facilitated by a simplified analytical model that expresses the net in-phase force feedback in terms of the admittance of the accumulator, thereby providing a frame of reference for the use of judgment in the design. Treating the effects of the fuel and oxidizer systems as independent and additive and reckoning force feedback at the structure modal frequency only permit a simple description of the primary mechanism. A novel feature of the model is that the effect of outflow perturbations on tank-bottom pressure is included in the net-thrust function.

INTRODUCTION

The type of instability that has come to be known as "pogo" consists of longitudinal oscillation occurring near the end of the thrust period in liquid-propelled rocket vehicles. The mechanism is a feedback loop in which propellant-flow oscillations driven by the structure produce thrust oscillations that, in turn, drive the structure. The pogo problem was studied in connection with the Gemini launch vehicle and satisfactory corrective devices were developed (refs. 1 and 2). Analytical models have been developed both for specific vehicles and for more general application, including a general algebraic model (ref. 3) and a general computer model (refs. 4 and 5).

Reported pogo occurrences have the following characteristics in common:

(1) The structure oscillates in the lowest-frequency mode in which the oscillation velocities of the engine and payload are opposite in phase, and the frequency of oscillation closely approximates the modal frequency.

(2) Pogo occurs during the last part of the thrust period, usually shortly before cutoff.

(3) Occurrence of pogo is associated with a condition of resonance or a near approach to resonance in the pump feed system of at least one propellant.

Various methods of preventing pogo have been proposed, including

(1) Increasing structural damping to make the system stable in spite of thrust feedback

(2) Changing ullage pressure to change pump gain and feed-system resonant frequency

(3) Increasing feedline area to increase pressure force at the pump inlet

(4) Use of a compliant device (accumulator) at the pump inlet to lower feedline resonant frequency

(5) Use of a volume-compensating device to reduce or eliminate input from the structure to the propellant system

(6) Use of compliant inserts or gas bubbles in the feedline to increase damping and lower resonant frequency

Of these methods, the pump-inlet accumulator is probably the most practical and economical. In its application the device has been designed to lower the fundamental resonance of the feed system to below the structure frequency and keep the second feed-system frequency above that of the structure throughout the thrust period. This method is satisfactory but may lead to overconservative requirements.

The model presented herein is the outcome of a quest for an analytical representation of pogo that would be simple enough to provide physical insight into the basic mechanism and realistic enough to be useful as an aid in establishing design requirements for accumulators. Exploratory calculations using a bipropellant model similar to that of reference 3 indicated that the feedback effects of the two propellant systems are roughly independent and additive. It became apparent that the model could be simplified greatly by neglecting the interaction between propellant systems, treating each as if there were no oscillation in the other. A simple model based on this assumption was developed in the hope that such a model, requiring a minimum of calculation and providing a simple description of the primary effect of accumulator parameters on propulsion feedback, would facilitate the selection of tentative design requirements and simplify the trial-and-error procedures required for optimization.

The model contains two major simplifying assumptions in addition to those usually found in pogo models: that the effects of the two propellant systems are independent and additive, and that stability at any time can be determined by calculating force feedback only at the modal frequency of the structure. Otherwise, this model is very similar to that of reference 3 except that the accumulator admittance is included explicitly and the equations are cast in a form designed to reveal the effect of accumulator admittance on net force feedback. A new feature in the present model is the inclusion of the contribution of the tank-bottom pressure oscillation to the retarding force exerted by the feed

system on the structure.

The model is intended primarily for use as a design tool. Precise stability analysis requires the use of a complete bipropellant model including the propellant interaction effect.

ANALYTICAL MODEL

Assumptions

The following assumptions are used in the development of the model:

(1) The problem may be treated as linear for small perturbations about steady-state values.

(2) Vehicle and propulsion-system parameters vary slowly with time and can be considered to be constant for sinusoidal-perturbation analysis at any given time.

(3) Oscillatory velocity and displacement of parts of the structure and flow perturbations in inlet lines are defined with respect to a reference system moving with the smoothed velocity and acceleration of the center of mass. Flow perturbations downstream from the pump inlet are defined with respect to the conduit.

(4) Compressibility is negligible between the pump inlet and the injector.

(5) Friction losses in inlet lines are negligible.

(6) Effective coupling between structure and propellant feed system occurs only upstream of the pump.

(7) Pump-inlet cavitation behaves as a pure compliance.

(8) In the pump equation, gain $(m + 1)$ is real, and resistance R is independent of frequency. (Symbols are defined in appendix A.)

(9) An adequate structure model exists, from which modal frequency ω_n, effective mass at gimbal point M_n, and mode-shape factors φ_n for selected structural elements may be calculated as a function of time for modes of interest. The structure model includes liquid in the propellant tanks, but the feedlines are empty. The lines are assumed to be closed at the tank bottom. Therefore, forces exerted by the liquid on the structure when the outflow oscillation is zero are included in the structure model.

(10) Forces applied to the structure by the propellant system do not modify the mode shapes.

In addition to the foregoing assumptions, which are common to most pogo models (refs. 3 and 4), the following special assumptions are used in the present model:

(1) The component of the tank-bottom pressure oscillation caused by propellant outflow oscillation has a negligible effect on the propellant-flow response to structure motion, but the resulting component of pressure force on the structure (not included in

the structure model) constitutes a significant part of the total reaction of the propellant system on the structure.

(2) Effects of the two propellant systems are independent and additive. Oscillation in either may be determined by assuming no oscillation in the other, and the sum of forces on the structure caused by both independently is not substantially different from the effect of both acting together.

This assumption permits a simple formulation of the basic feedback mechanism unobscured by confusing second-order effects. It is justifiable because the determination of requirements for a corrective device requires that attention be focused on the primary effect of one propellant system.

(3) The structure is massive and very lightly damped; therefore, the thrust-feedback function calculated at the modal frequency and only at this frequency may be used to determine stability. (This assumption represents a departure from the point of view of control theory because frequency is not regarded as an independent variable.) The logical basis for this assumption is more fully developed in the following section.

Stability Criterion

A condition of neutral stability exists if, at any frequency, the mechanical impedance of the structure at the gimbal point equals the net-thrust transfer function. The mechanical impedance Z_m is the complex ratio of driving force to velocity required for steady-state sinusoidal oscillation. It may be calculated as a function of frequency from the structure model. The net-thrust function $T_N/\dot{x}_g$ is made up of the engine thrust oscillation minus the effect of forces applied to the structure as a result of flow oscillations in the propellant lines. It is expressed as the ratio of effective force to velocity at the gimbal point.

The general nature of the variation in magnitude of these transfer functions with frequency at a particular time is illustrated in figure 1(a). The mechanical impedance is characterized by a very sharp minimum at the natural frequency of each structural mode. For bipropellant systems the net-thrust function generally has not more than two peaks, and these are broad compared to the narrow-band minima of Z_m. Since $|T_N/\dot{x}_g|$ must exceed $|Z_m|$ for instability, it is clear that oscillation is possible only at frequencies very close to the natural frequency of a structural mode (modal frequency). Moreover, the minimum value of Z_m is ordinarily least at the lowest-frequency mode; therefore, the higher modes are less likely to be unstable.

A comparison of the net-thrust and mechanical-impedance functions in the neighborhood of a modal frequency ω_n is shown in more detail in figure 1(b), in which the real and imaginary parts of both transfer functions are shown as a function of ω/ω_n.

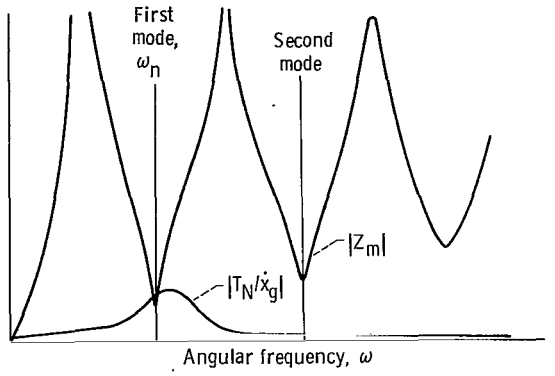

(a) General nature of the variation.

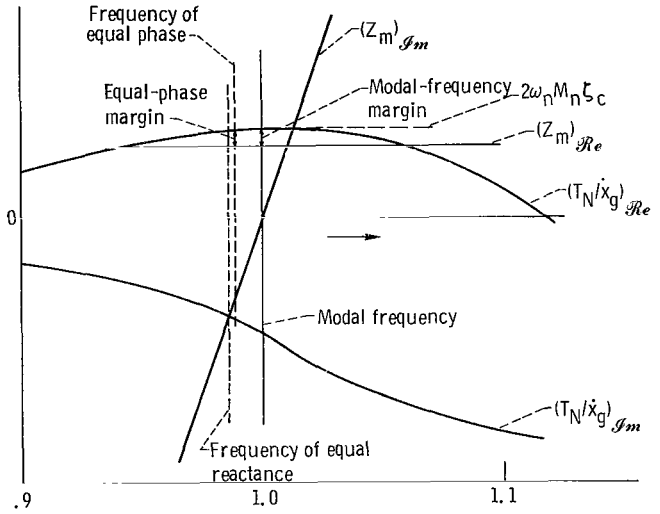

Ratio of angular frequency to angular modal frequency, ω/ω_n

(b) Detailed comparison.

Figure 1. - Comparison of net-thrust transfer function and gimbal-point mechanical impedance.

The criterion for stability is that the system is stable if the real part of $T_N/\dot{x}_g$ is less than the real part of Z_m at the frequency at which the imaginary parts are equal. Because of the very rapid change in the imaginary part of Z_m with frequency (a consequence of large mass and very light damping), only a small error is introduced if the comparison of the real parts of Z_m and $T_N/\dot{x}_g$ is made at the modal frequency ω_n instead of the frequency of phase coincidence. This is an important simplification because it eliminates the use of frequency as a scanning variable. The net-thrust function at ω_n may be calculated as a function of a single independent variable, time.

The mechanical impedance at the modal frequency is

$$Z_m = 2\omega_n M_n \zeta_n \tag{1}$$

The frequency and modal mass M_n (with respect to the gimbal point) are obtained from the spring-mass model of the structure, but the damping factor ζ_n must be obtained from test data or estimated from experience with similar vehicles. Because of uncertainty in ζ_n, it is convenient to present the results of stability analyses in terms of the damping factor required for neutral stability ζ_C.

On the basis of the approximate stability criterion, ζ_C is given by

$$\zeta_C = \frac{\left(\frac{T_N}{\dot{x}_g}\right)_{Re}}{2\omega_n M_n} \tag{2}$$

when $T_N/\dot{x}_g$ is evaluated at the modal frequency ω_n. The assumption that the effects of the two propellant systems are independent and additive permits the separation of the net-thrust function into two components

$$\frac{T_N}{\dot{x}_g} = \frac{F_o}{\dot{x}_g} + \frac{F_f}{\dot{x}_g} \tag{3}$$

For either propellant acting alone, the thrust function is conveniently expressed in dimensionless form in terms of two force-feedback parameters ξ and ν defined by the following equation:

$$\xi + i\nu \frac{1}{2\omega_n M_n} \frac{F}{\dot{x}_g} \tag{4}$$

In this equation F is the net effective force at the gimbal point resulting from oscillations in one propellant system at the frequency ω_n. Since only the real part of the thrust function appears in equation (2), the damping factor required for neutral stability is

$$\zeta_C = \xi_f + \xi_o \tag{5}$$

Expressions for ξ in terms of vehicle and propellant-system parameters are to be determined from an analysis of the propulsion system.

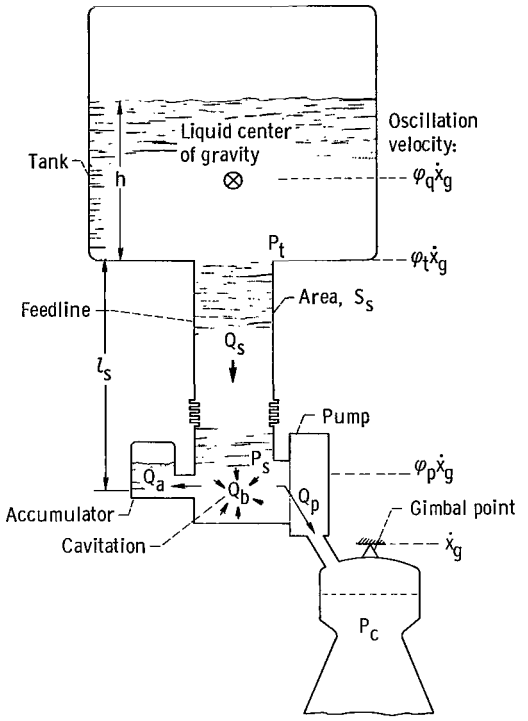

Figure 2. - Schematic diagram of system.

Inlet System

A simple form of propellant system is illustrated in figure 2. It consists of a tank, a short feedline, a pump, a discharge line, and an injector. An accumulator is attached at the pump inlet for the purpose of stabilizing the system. The admittance of the accumulator is represented in general form by

$$Y_a = G_a + iB_a \tag{6}$$

The thrust chamber is assumed to move with the gimbal-point oscillation velocity $\dot{x}_g$ (positive forward). The structure oscillates at a modal frequency ω_n. The ratio of amplitude at any point to the gimbal-point amplitude is expressed by the mode-shape factor φ. In the model of the structure the liquid in the tank is represented by a single lumped mass having the oscillation velocity $\varphi_q \dot{x}_g$ when the feedline is closed at the entrance. With the feedline open, the flow perturbation entering the feedline is Q_s; and, therefore, the oscillation velocity of the liquid center of mass becomes

$$\dot{x}_q = \varphi_q \dot{x}_g - \frac{\varphi_q}{\varphi_t} \frac{Q_s}{S_t} \tag{7}$$

The pressure perturbation at the entrance to the feedline is, therefore,

$$P_t = i\omega_n \rho h \varphi_q \dot{x}_g - \frac{i\omega_n \rho h \varphi_q}{S_t \varphi_t} Q_s \tag{8}$$

The second term is small compared to the first and may be neglected at this point, giving

$$P_t = i\omega_n \rho h \varphi_q \dot{x}_g \tag{9}$$

(It is usually assumed that the tank-bottom pressure perturbation is independent of the flow perturbation in the line (refs. 1 and 3). Since $Q_s/S_t \ll \dot{x}_g$, this assumption is valid when the purpose is to determine the feed-system response to structure oscillation. However, if it is desired to determine the forces on the structure resulting from oscillation in the feed system, the flow-dependent term is important because the component of pump suction pressure in phase with $\dot{x}_t$ produces a quadrature component in Q_s that gives rise to a component of P_t in phase with and opposing the structure oscillation velocity.)

Since the feedline is short compared to a/ω_n and is terminated in a low impedance at the tank, it may be treated as a lumped inertance given by

$$L_s = \frac{\rho l_s}{S_s} \tag{10}$$

The flow perturbation in the line (positive aft) is related to the pressure difference as follows

$$Q_s = \frac{S_s}{i\omega_n \rho l_s} (P_t - P_s) \tag{11}$$

The compliance C_b of cavitation in the pump inlet is the rate of decrease in total volume of bubbles with increasing pump suction pressure. The response of volume to

pressure is not purely compliant but is characterized also by an inertial effect arising from the acceleration of liquid about the bubbles and a lag resulting from heat transfer associated with evaporation and condensation. Since these effects cannot be estimated reliably and are thought to be minor, it is assumed that the cavitation behaves as a pure compliance, and the flow into the compliance is given by

$$Q_b = i\omega_n C_b P_s \tag{12}$$

An accumulator having an admittance Y_a (a complex function of frequency and operating pressure) is attached at the pump inlet. The flow into the accumulator is

$$Q_a = Y_a P_s \tag{13}$$

The flow perturbation entering the pump is defined with respect to the pump casing; therefore, the flow equivalent of the pump oscillation velocity is included in the equation for Q_p.

$$Q_p = Q_s + S_s \varphi_p \dot{x}_g - Q_b - Q_a \tag{14}$$

Substitution from equations (9), (11), (12), and (13) into equation (14) yields the low-pressure feed-system equation

$$Q_p = A\dot{x}_g - YP_s = S_s\left(\varphi_p + \frac{h}{l_s}\varphi_q\right)\dot{x}_g - \left(Y_a + i\omega_n C_b + \frac{S_s}{i\omega_n \rho l_s}\right)P_s \tag{15}$$

This equation applies to the configuration of figure 2 when $\omega_n l_s/a < 0.1\pi$. In general, an analysis of any practical low-pressure feed system yields an expression of this form. For a longer line such as analyzed in reference 6 with $0.1\pi < \omega_n l_s/a < 0.9\pi$, parameters A and Y are given by

$$A = S_s\left[\varphi_p + \varphi_q \frac{h}{l_s}\left(\frac{\frac{\omega_n l_s}{a}}{\sin\frac{\omega_n l_s}{a}}\right)\right] \tag{16}$$

$$Y = Y_a + i\omega_n C_b + \frac{S_s}{i\omega_n \rho l_s} \frac{\omega_n l_s}{a} \cot \frac{\omega_n l_s}{a} \tag{17}$$

For most systems A is real, and Y is imaginary for the unmodified feed system (damping negligible in inlet line). With the accumulator attached, the combined admittance may be written as the sum of the accumulator admittance $G_a + iB_a$ and the unmodified system admittance iB_u.

$$Y = G_a + i(B_a + B_u) \tag{18}$$

Equation (15) shows that the system behaves as if the effect of structure motion were to inject into the feed system at the lower end of the line a flow oscillation equivalent to that produced by a piston of area A moving with the gimbal-point velocity $\dot{x}_g$. The reaction of the feed system on the structure is, therefore, equivalent to a retarding force acting at the gimbal point given by

$$F_R = AP_s \tag{19}$$

The expression AP_s includes the significant effect on the structure caused by the component of tank-bottom pressure that results from propellant outflow oscillations. This fact is verified for the configuration of figure 2 as follows: Equations (8) and (11) are used to obtain an expression for P_t in terms of $\dot{x}_g$ and P_s without using the approximation of equation (9).

$$P_t = \frac{i\omega\rho h\varphi_q \dot{x}_g + \frac{h}{l}\frac{S_s}{S_t}\frac{\varphi_q}{\varphi_t} P_s}{1 + \frac{h}{l}\frac{S_s}{S_t}\frac{\varphi_q}{\varphi_t}}$$

The above denominator is a scaler quantity that may vary only from 1.0 to about 1.1 in extreme cases; therefore,

$$P_t \cong i\omega\rho h\varphi_q \dot{x}_g + \frac{h}{l}\frac{S_s}{S_t}\frac{\varphi_q}{\varphi_t} P_s$$

The first term is included in the structure model, and the additional component of tank-bottom pressure due to propellant flow oscillations is given by

$$P_t' \cong \frac{h}{l} \frac{S_s}{S_t} \frac{\varphi_q}{\varphi_t} P_s$$

and the effective propellant-system reaction at the gimbal point is

$$F_R = S_s P_s \varphi_p + S_t P_t' \varphi_t = S_s \left(\varphi_p + \frac{h}{l} \varphi_q \right) P_s = A P_s$$

In order to obtain expressions for the pump-flow and suction-pressure transfer functions before proceeding with the analysis of the discharge system, it is assumed at this point that the relation between pump throughflow and suction pressure may be represented by an effective impedance (the assumption of independence of fuel and oxidizer systems is implied),

$$Z' = \frac{P_s}{Q_p} \tag{20}$$

Equations (15) and (20) describe a dividing network for which the ratio of output to input is given by

$$\frac{Q_p}{A\dot{x}_g} = \frac{1}{1 + YZ'} \tag{21}$$

The pump-flow transfer function is

$$\frac{Q_p}{\dot{x}_g} = \frac{A}{1 + YZ'} \tag{22}$$

And the suction-pressure transfer function is

$$\frac{P_s}{\dot{x}_g} = \frac{AZ'}{1 + YZ'} \tag{23}$$

Pump and Engine

The dynamic behavior of the pump is represented by an equation of the form (ref. 1).

$$P_d = (m + 1)P_s - Z_p Q_p \tag{24}$$

Limited unpublished results from tests conducted at Lewis indicate that the real part of Z_p may be frequency-dependent and that $m + 1$ may be complex. However, for the purpose of the present analysis, it is assumed that $m + 1$ is real and that Z_p can be represented by

$$Z_p = R_p + i\omega L_p \tag{25}$$

In the absence of dynamic test data, $m + 1$ and R_p may be estimated from steady-state performance data (see ref. 1), and a rough approximation of L_p may be calculated from the internal geometry of the pump.

Since the injector resistance is small compared to the characteristic impedance of the discharge line, it is assumed that the system downstream of the pump is incompressible; therefore, Q_p represents also the flow perturbation at the injector. The discharge line and injector are represented by a lumped impedance in the pressure equation:

$$P_d = P_c + Z_d Q_p \tag{26}$$

where

$$Z_d = R_d + i\omega L_d$$

Some uncertainty exists concerning line resistance to oscillatory flow when the mean throughflow is in the turbulent regime. Linearization of the steady-state pressure-flow relation is valid only if the period of oscillation is long compared with the time required to establish the steady-state turbulent-flow velocity profile.

An equation for the pump-inlet pressure perturbation is obtained from equations (24) and (26)

$$P_s = \frac{Z_p + Z_d}{m + 1} Q_p + \frac{1}{m + 1} P_c \tag{27}$$

The pressure oscillation in the thrust chamber results from flow oscillations of fuel and oxidizer and is characterized by a time lag that is small compared to $1/\omega_n$. The average combustion delay time is added to the first-order lag of the chamber volume to obtain the time constant τ_c. The pressure oscillation is given by

$$P_c = \frac{H_f Q_{pf} + H_o Q_{po}}{1 + i\omega_n \tau_c} \tag{28}$$

The partial-resistance coefficients H_o and H_f are defined as the zero-frequency variation of chamber pressure with propellant flow for one propellant, assuming steady flow of the other. These coefficients include the effect of variation in oxidant-fuel ratio on characteristic velocity. They may be determined from engine performance data as described in reference 3. (In the notation of ref. 3, H is represented by $C^*\rho/A_t g$.)

In order to calculate an effective impedance for each propellant looking from the injector into the thrust chamber, the interaction implied in equation (28) is neglected, and oscillation in only one propellant system is assumed. Noting also that $\omega_n^2 \tau_c^2 << 1$, the effective impedance is, for either propellant,

$$\frac{P_c}{Q_p} = H(1 - i\omega_n \tau_c) \tag{29}$$

The effective pump-inlet impedance Z' required for use in equations (22) and (23) is obtained from equations (27) and (29)

$$\frac{P_s}{Q_p} = Z' = R' + iX' \tag{30}$$

where

$$R' = \frac{1}{m + 1}(R_p + R_d + H)$$

$$X' = \frac{\omega_n}{m + 1}(L_p + L_d - H\tau_c)$$

Net-Thrust Transfer Function

The transfer function relating chamber pressure to gimbal-point oscillation velocity is obtained by assuming that the effects of the two propellants are additive, though each is determined as if the other were zero. Using equation (22) in equation (28),

$$\frac{P_c}{\dot{x}_g} = \left[\frac{HA}{(1 + i\omega\tau_c)(1 + YZ')}\right]_f + \left[\frac{HA}{(1 + i\omega\tau_c)(1 + YZ')}\right]_o \tag{31}$$

The driving force on the structure at the gimbal point produced by the chamber-pressure oscillation is $S_E P_c$, where S_E is the ratio of mean thrust to mean chamber pressure. Because the reaction of each feed system on the structure is equivalent to a retarding force AP_s at the gimbal point (eq. (19)), the net-thrust perturbation is

$$T_N = S_E P_c - A_f P_{sf} - A_o P_{so} \tag{32}$$

The chamber-pressure and suction-pressure transfer functions (eqs. (31) and (23)) are used in equation (32) to obtain the net-thrust transfer function

$$\frac{T_N}{\dot{x}_g} = \left[\frac{S_E AH}{(1 + i\omega_n\tau_c)(1 + YZ')} - \frac{A^2 Z'}{1 + YZ'}\right]_f + \left[\frac{S_E AH}{(1 + i\omega_n\tau_c)(1 + YZ')} - \frac{A^2 Z'}{1 + YZ'}\right]_o \tag{33}$$

This equation is in the same form as equation (3); each term represents the thrust function for one propellant. In order to show explicitly the effect of an accumulator, equation (18) is used for Y in equation (33), and the dimensionless force-feedback function for one propellant (eq. (4)) is written in a form intended to reveal the effect of G_a and B_a. For either propellant,

$$\xi + i\nu = \frac{S_E AH}{2\omega_n M_n}\left(\frac{1 - i\dfrac{X'}{R'}}{1 + i\omega_n\tau_c} - \frac{A|Z'|^2}{S_E HR'}\right)\left(\frac{R'}{R' + G_a|Z'|^2}\right)\left[\frac{1}{1 - i\dfrac{X' - (B_a + B_u)|Z'|^2}{R' + G_a|Z'|^2}}\right] \tag{34}$$

In order to facilitate the intelligent selection of G_a and B_a, equation (34) is transformed in a manner intended to reveal more clearly the effect of various system parameters

$$\frac{\xi + i\nu}{K\lambda} = \Omega e^{i(\theta + \psi)} \cos \psi \tag{35}$$

This form was obtained by representing the four factors in equation (34) as follows:

$$\frac{S_E A H}{2\omega_n M_n} = K \tag{36}$$

$$\frac{R'}{R' + G_a |Z'|^2} = \lambda \tag{37}$$

$$\frac{1 - i\dfrac{X'}{R'}}{1 + i\omega_n \tau_c} - \frac{A|Z'|^2}{S_E H R'} = \Omega e^{i\theta} \tag{38}$$

$$\frac{1}{1 - i\dfrac{X' - (B_a + B_u)|Z'|^2}{R' + G_a|Z'|^2}} = \frac{1}{1 - i \tan \psi} \equiv e^{i\psi} \cos \psi \tag{39}$$

The parameter K is a scale factor that expresses, in units of ζ, the gross thrust for direct in-phase coupling as would be realized with undamped inlet-system resonance, pure resistance on the discharge side, and no lag. The factor λ describes the reduction in feedback amplitude caused by damping in the accumulator. The complex factor $\Omega e^{i\theta}$ represents, in polar form, the combined effects of the phase shift caused by thrust-chamber lag and discharge-system reactance and the relative back force exerted by the inlet system. The effect of inlet-system resonance is described in terms of the detuning angle ψ.

Representation of the normalized force-feedback function $(\xi + i\nu)/K\lambda$ in the complex plane (fig. 3) illustrates the effect of Ω, θ, and ψ. Parameters Ω and θ are independent of resonance conditions in the feed system. Therefore, a single point represents $\Omega e^{i\theta}$ at a given time for all possible combinations of B_a and G_a. The locus

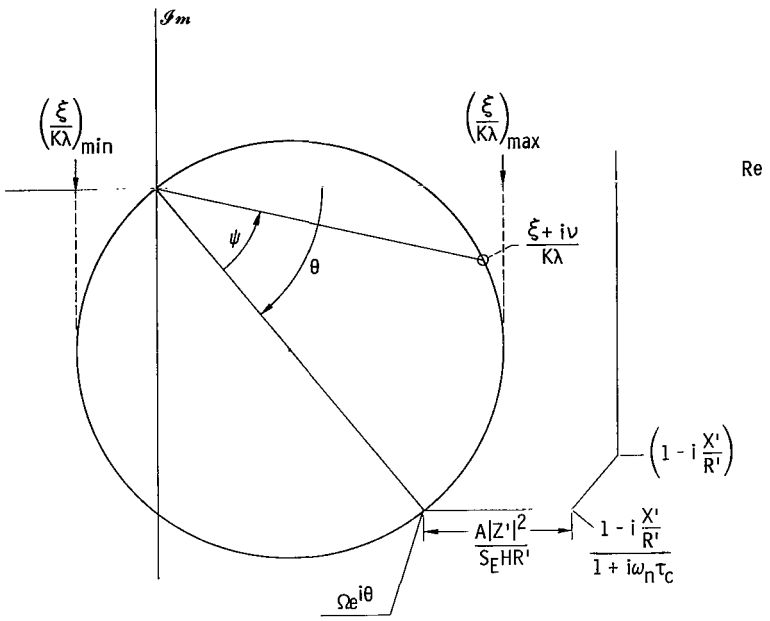

Figure 3. - Complex-plane representation of normalized force-feedback function $(\xi + i\nu)/K\lambda$.

of $(\xi + i\nu)/K\lambda$ is a circle constructed on the radius vector $\Omega e^{i\theta}$ as a diameter. For large negative values of $B_a + B_u$, the angle ψ approaches 90^o. With increasing $B_a + B_u$, ψ decreases, passing through zero when $B_a + B_u = X'/|Z'|^2$ and approaching -90^o at large positive values of $B_a + B_u$. The horizontal extent of the circle defines the limits within which $\xi/K\lambda$ may vary with changes in inlet-system admittance, and since λ cannot exceed 1, the limits of ξ are

$$\xi_{max} = \frac{K\Omega}{2}(\cos\theta + 1) \tag{40}$$

$$\xi_{min} = \frac{K\Omega}{2}(\cos\theta - 1) \tag{41}$$

The variation of ξ between these limits is obtained by taking the real part of equation (35).

$$\xi = K\lambda\Omega \cos(\theta + \psi) \cos\psi \tag{42}$$

APPLICATION

Recall that the structure damping factor required for neutral stability is obtained by evaluating ξ for both propellants at the structure modal frequency ω_n.

$$\zeta_C = \xi_f + \xi_o \tag{5}$$

Since the accumulator conductance G_a and susceptance B_a are instrumental in determining ψ and λ, the variation of ξ between the limits given by equations (40) and (41) can be influenced by specifying G_a and B_a, and ξ may be confined within allowable limits.

Effect of Accumulator on Thrust-Feedback Function

The variation of ξ with the combined inlet-system admittance $Y = G_a + i(B_a + B_u)$ can be understood by means of the complex-plane diagram (fig. 3). For the unmodified system, $Y = B_u$ and $\lambda = 1$. As B_u increases from large negative values, the detuning angle ψ decreases from near 90^o and the point representing $(\xi + i\nu)K\lambda$ moves clockwise along the circle. The maximum value of $\xi/K\lambda$ occurs when $\psi = -\theta/2$, and the minimum when $\psi = -90^o - (\theta/2)$. The variation of ξ between its limits depends on the variation with time of the modal frequency ω_n in relation to the inlet-system frequency ω_s (at which $B = 0$). Two examples are shown in figure 4. Figure 4(a) represents a short feedline with pump-inlet cavitation increasing near the end of firing. The inlet-system frequency decreases, crossing the structure frequency. In this case ξ starts small and positive, increases to the upper limit as the frequencies cross, decreases quickly to the lower limit, and rises slowly toward zero. Figure 4(b) represents a long feedline with decreasing cavitation (increasing P_s). The sequence of events is reversed as ω_s crosses ω_n from below.

Also shown in figure 4 is the effect of small undamped and lightly damped accumulators. In both cases the resonant frequency of the accumulator is higher than ω_n, making B_a positive at all times. In figure 4(a), the maximum of ξ occurs earlier in flight as a result of lowering the inlet-system frequency ω_s. In figure 4(b), the pattern of variation in ξ is shifted in the opposite direction. With damping, the peak value of ξ is below the limit given by equation (40), and the system passes through resonance more slowly.

If the inlet-system frequency tends to track the structure frequency as in figure 4(b), a small undamped accumulator is sufficient to provide adequate frequency separation at all times. The system represented by figure 4(a) poses a more difficult problem because

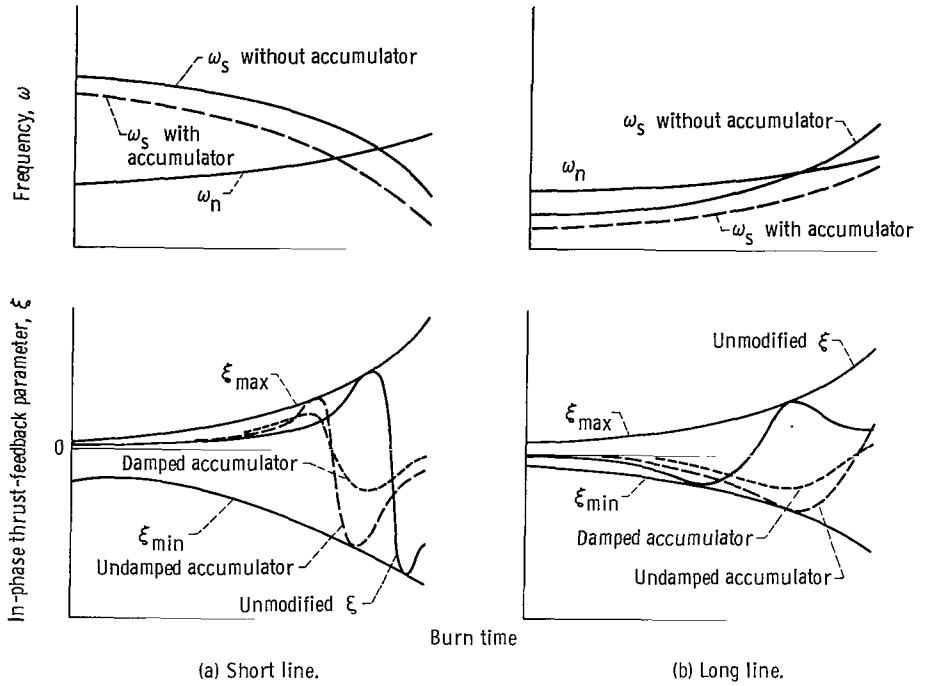

(a) Short line. (b) Long line.

Figure 4. - Effect of accumulator on thrust feedback.

a very large accumulator would be required to provide frequency separation at lift-off. The situation is not as bad as it looks, however, because ω_s is much higher than ω_n only if the feedline is short. And a short line implies a large value of A in the early part of the thrust period. In these circumstances the back force AP_s is large, and ξ_{max} is so small that resonance may be allowed during the early part of the thrust period. In this case damping in the accumulator is advantageous because it decreases the peak value of ξ.

Accumulator Design Considerations

Because of the wide variety of possible relations among several parameters, it is not feasible to propose a general procedure for selecting design conditions. Optimal design requires judgment, experience, and at least a minimum of trial-and-error procedure. The present model is intended to aid in the design procedure in two ways: (1) by providing a framework within which the designer may exercise judgment in selecting a design point, and (2) by providing a means of verifying tentative designs by means of relatively simple calculations.

The pattern of in-phase force feedback for one propellant system is defined by the curve of ξ as a function of time. Addition of an accumulator to the system gives rise

to a different curve, but all such curves are included between the envelopes defined by ξ_{max} and ξ_{min}. Examination of the envelope curves and the unmodified ξ curve for both propellant systems provides the information required to decide whether either or both systems require modification.

The curves of ξ in figure 4 show the general nature of changes caused by increasing B. These curves and a study of the relation between figures 3 and 4 should suggest the character of changes in ξ to be expected for systems different from those illustrated in figure 4. Based on a qualitative understanding of the shape of realizable ξ curves, a single critical point can be selected for design. Examples of the type of design condition that may be specified are the latest time at which ξ is allowed to reach the upper limit or the time at which ξ is zero. Either of these conditions defines a limiting value of $B_a + B_u$ at the selected time. The design condition also may be specified as a limit less than ξ_{max} for a peak value of ξ at a given time, defining also a minimum required value of G_a.

Based on the design condition, the accumulator configuration and tentative values of the circuit elements are selected. Various configurations are possible, and a variety of admittance-frequency characteristics are realizable by combining compliance C, inertance L, and resistance R in various ways. The accumulator conductance G_a and susceptance B_a are calculated for the equivalent circuit by methods applicable to electrical networks. Some possible configurations and the relation between the ideal elements R, L, and C and their physical counterparts are discussed in appendix B.

The tentative design is used to calculate G_a and B_a as a function of time, taking into account variations of circuit elements and frequency ω_n with time, and these values are used to generate a curve of ξ for the modified system. Additional checkout calculations can be made by using upper and lower limits for uncertain parameters.

Similar procedures may be applied to the second or higher structural modes if doubt exists as to their stability. The fact that higher-mode oscillation has not been observed suggests the possibility that ξ_{max} is generally less than ζ_n except in the lowest mode.

A specific example, illustrating some possible design procedures, is presented in appendix C.

CONCLUDING REMARKS

Interaction between fuel and oxidizer systems (due to the thrust chamber being common to both) has been neglected in the present model, as has the frequency shift caused by the quadrature component of net-thrust feedback. By means of these approximations, the model is reduced to a simple form that reveals the basic feedback mechanism unobscured by second-order effects, and indicates clearly the changes in thrust

feedback that may be realized by means of pump-inlet accumulators. This model includes also an improved method of reckoning the effective force exerted on the structure by the propellant systems, eliminating the error resulting from the assumption (in previous models) that tank-bottom pressure is independent of perturbations in outlet flow.

Because of the simplifying assumptions used in its development and the difficulty anticipated in determining critical parameters such as pump gain and compliance, the model is not suitable for predicting instability in cases that may be marginal. However, this model was developed with a view to a practical solution of the longitudinal-oscillation problem. From this viewpoint an exact determination of stability limits is not required because prevention of instability (pogo), rather than prediction, is the aim. If prevention of pogo is deemed of sufficient importance to warrant modification of the propellant systems, the model may be used to define the required admittance of pump-inlet accumulators for fuel or oxidizer or both. The model may be used also to check the stability of the modified system, since prudent design requires that the in-phase thrust feedback be so small that moderate percentage errors in its determination would be tolerable.

Lewis Research Center,
National Aeronautics and Space Administration,
Cleveland, Ohio, June 2, 1969,
120-27-04-27-22.

APPENDIX A

SYMBOLS

A	input coefficient, $in.^2$; m^2
a	sonic speed, in./sec; m/sec
B	susceptance, $in.^5$/lb-sec; m^5/N-sec
C	compliance, $in.^5$/lb; m^5/N
F	force, lb; N
G	conductance, $in.^5$/lb-sec; m^5/N-sec
H	thrust-chamber partial-resistance coefficient, lb-sec/$in.^5$; N-sec/m^5
h	liquid level, in.; m
i	$\sqrt{-1}$
K	force-feedback scale factor, nondimensional
k	kinematic factor (see ref. 6), nondimensional
L	inertance, lb-sec^2/$in.^5$; kg/m^4
ℓ	length, in.; m
ℓ'	effective length, in.; m
M	effective (modal) mass, lb-sec^2/in.; kg
m + 1	pump gain, nondimensional
P	pressure, psi; N/m^2
Q	volume flow rate, $in.^3$/sec; m^3/sec
R	resistance, lb-sec/$in.^5$; N-sec/m^5
R'	effective resistance looking into pump
r	radius, in.; m
S	area, $in.^2$; m^2
T_N	net-thrust perturbation, lb; N
V	volume, $in.^3$; m^3
v	velocity, in./sec; m/sec
X	reactance, lb-sec/$in.^5$; N-sec/m^5
X'	effective reactance looking into pump, lb-sec/$in.^5$; N-sec/m^5
x	displacement, in.; m
$\dot{x}$	velocity, in./sec; m/sec
$\ddot{x}$	acceleration, in./sec^2; m/sec^2
Y	admittance, $in.^5$/lb-sec; m^5/N-sec
Z	impedance, lb-sec/$in.^5$; N-sec/m^5
Z'	effective impedance looking into pump, lb-sec/$in.^5$; N-sec/m^5
γ	ratio of specific heats
ζ	damping factor, nondimensional
θ	force-feedback phase angle at resonance, deg; rad
κ	spring rate, lb/in.; N/m
λ	force-feedback amplitude reduction factor, nondimensional
ν	quadrature component of force-feedback function, nondimensional
ξ	in-phase component of force-feedback function, nondimensional

ρ	density, lb-sec^2/in^4; kg/m^3
σ	pressure-loss coefficient, nondimensional
τ	time constant, sec
φ	mode-shape factor (gimbal point = 1.0), nondimensional
ψ	force-feedback detuning angle, deg; rad
Ω	force-feedback amplitude factor, nondimensional
ω	angular frequency, sec^{-1}

Subscripts:

a	accumulator
b	cavitation
C	critical (stability boundary)
c	thrust chamber
d	discharge system
f	fuel system
g	gimbal point
h	thermal
$\mathcal{I}m$	imaginary part
m	mechanical
n	modal
nl	nonlinear
o	oxidizer
p	pump
q	liquid center of mass
R	propellant system reaction
$\mathcal{R}e$	real part
s	suction line or pump inlet station
t	tank
u	unmodified
w	working
1,2,3	circuit elements

APPENDIX B

SOME PRACTICAL ASPECTS OF ACCUMULATOR DESIGN

Accumulator Configurations

Perhaps the simplest form of accumulator consists of a volume of noncondensable gas connected to the propellant line by a short liquid-filled duct, as shown in figure 5. If the propellant is a liquid storable at ambient temperature and in which air is not highly soluble, the gas charge may consist of the air entrapped when the system is filled (fig. 5(a)). Otherwise, gas may be drawn from existing storage on the vehicle or from a local storage tank, as shown in figure 5(b). Storage within the accumulator in a flexible container, as in figure 5(c), is another possibility. If the gas is initially at atmospheric pressure, the entrapped volume must be large enough to allow for compression to operating pressure. Moreover, the possibility of some loss of gas during the starting transient must be examined.

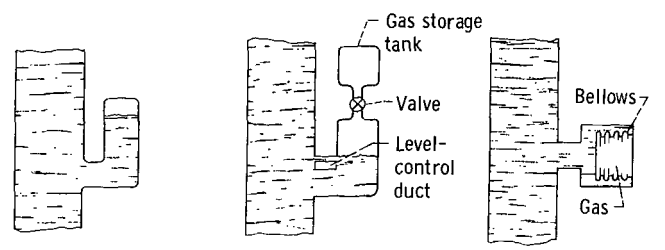

Figure 5. - Accumulator configurations.

Relatively larger working volume may be obtained by using the arrangement illustrated in figure 5(b), in which the gas charge is stored under pressure in a separate chamber. The connecting valve is opened after operating pressure is established. The resistance and inertial reactance of the connecting tube and valve can readily be made negligible compared to the compliant reactance of the gas remaining in the storage chamber. Thereby the effective compliance is made equal to that of the total volume of gas in both chambers. If damping is desired, use of a porous plug in the connecting tube provides a convenient means of realizing approximately linear resistance. Use of the connecting tube as an inertance element is not considered to be practical because of the low density of the gas. If the pressure decreases with time, it may be desirable to con-

trol the liquid level at a point at least one radius above the top of the duct to allow for finite oscillations without getting gas in the main duct. Liquid-level control may be accomplished by the use of a small secondary duct large enough to permit the escape of excess gas but so small that its impedance is much greater than that of the main duct (fig. 5(b)).

The foregoing are only examples of some devices that might be employed. Actual design requires familiarity with the particular propellant system and associated hardware.

Physical Elements

The parameters that must be realized within specified limits are the susceptance B_a and conductance G_a. These parameters can be determined as a function of time at operating pressure and structure modal frequency if the device can be represented by a fluid circuit consisting of approximately linear inertance, compliance, and resistance. Various physical elements that may be employed are represented by corresponding combinations of ideal circuit elements, as shown in figure 6.

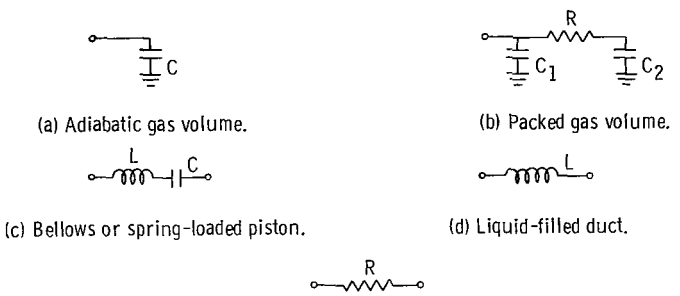

Figure 6. - Circuit representation of elements.

Adiabatic gas volume. - If the thermal time constant of the gas in the enclosure is much longer than the period of oscillation, the gas may be represented as a simple compliance proportional to the working volume

$$C = \frac{V_w}{\gamma P} \tag{B1}$$

At finite oscillation levels the nonlinearity of the pressure-volume relation introduces

harmonic distortion, but the effective value of compliance at the fundamental frequency is not strongly dependent on amplitude. Compliance from gas compressibility always acts in the circuit as a shunt to ground.

Packed gas volume. - If special means are provided to promote heat transfer to and from the gas, as by packing the volume with a material such as steel wool or fine wire and making the heat capacity of the solid large compared to that of the gas, the dynamic behavior is represented by the circuit of figure 6(b). The adiabatic compliance is represented by C_1, $C_1 + C_2$ is the isothermal compliance, and $RC_2 = \tau_h$ is the thermal time constant. Damping is significant at the modal frequency if $\tau_h \omega_n$ is in the neighborhood of 1. This means of providing resistance is desirable because the admittance is approximately independent of the flow-oscillation amplitude.

Bellows or piston. - A bellows or spring-loaded piston is represented by a compliance and an inertance in series, as shown in figure 6(c). The compliance is

$$C = \frac{S^2}{\kappa} \tag{B2}$$

where S is the effective area dV/dx and κ the spring rate dF/dx. The inertance is

$$L = \frac{M}{S^2} \tag{B3}$$

where M is the effective mass (e.g., the free end plus one-third of the convolutions of a bellows).

Liquid-filled duct. - The inertance of the liquid between the compliance and the propellant stream is probably the most difficult element to estimate accurately. For a straight circular duct of length l, cross-section area S, and radius r opening at both ends into large volumes of placid liquid, the inertance is

$$L = \frac{\rho l'}{S} \tag{B4}$$

where $l' = l + 2\Delta l$ and $\Delta l \cong 0.85\, r$.

The end corrections Δl represent the inertial effect of the liquid beyond the ends of the duct expressed as an equivalent extra length. The same equation applies approximately to curved ducts, l being the centerline length, when the radius of curvature of the centerline is greater than about $2r$. For tapered ducts, $\rho l/S$ is replaced by $\int \rho/S \, dl$.

Where the duct joins the propellant system, the main stream moves past the junction

at high speed, and the influence of the strong shear layer on the end correction cannot be determined analytically. In the absence of experimental data for liquid systems, uncertainty is unavoidable, but some basis for a qualitative estimate is found in the results of a study of the frequency shift of Helmholtz-resonator-type sound absorbers with increasing flow velocity in an air duct (ref. 7). It was found that the effective inertance of holes in a thin plate decreases at high tangential velocities to about 37 percent of its theoretical value (1.7 r). If this result is interpreted as a change in only the outside Δl, it would indicate a value less than zero. Intuitively, it appears unreasonable, with a duct of finite length, to have a negative end correction. But the result suggests strongly that the high velocity past the opening greatly reduces the end correction. It is suggested, therefore, that an end correction of zero be used for design calculations with a generous allowance for uncertainty.

No definite rules can be given for estimating the inertance within the accumulator from the duct to the gas volume. If a large area change occurs, the standard end correction (0.85 r) is a good approximation. Otherwise, an estimate of effective cross-sectional area as a function of axial length may be used as a basis for calculation.

Resistance elements. - Since the flow in and out of the accumulator is entirely oscillatory, the action of a resistance element having a square-law characteristic is strongly nonlinear, the effective resistance increasing with the first power of the flow amplitude. Because of the difficulty in predicting characteristics under operating conditions with variable resistance, and because of the frightening possibility that high effective resistance might in some circumstances prevent recovery from transient structural oscillations, it is important that resistance elements be as nearly linear as practicable.

Linearity of resistance may be assured by using resistance elements in which laminar flow prevails at the largest flow-oscillation amplitude likely to result from extraneous disturbances. A practical form of resistance element consists of a slab, plug, or sheet of porous material with a great number of small flow channels acting in parallel. Determination of the required combination of area, thickness, pore size, and flow-area fraction must be based on test data or reliable specifications for the material. Use of a porous-metal element as a linear resistance is discussed in reference 8.

Duct Area Requirement

Another problem that requires examination is the effect of nonlinear resistance caused by duct entrance and exit losses at high oscillation amplitude. If the duct contains a linear resistance element, the duct area will, in all probability, be large enough to make the nonlinear resistance negligible at any reasonable oscillation amplitude. However, if the accumulator is designed for undamped operation, or if a compound accumulator with

resistance in the gas-filled connecting tube or some other arrangement using an unobstructed main duct is contemplated, the nonlinear resistance imposes a minimum area requirement.

A relation between the effective nonlinear duct resistance R and the accumulator flow amplitude is obtained by applying the square-law pressure-drop relation to a sinusoidal flow oscillation (see ref. 9).

$$R_{nl} = \frac{4\sigma}{3\pi} \frac{\rho Q}{S^2} \tag{B5}$$

Experimental values of the pressure-loss coefficient σ (reciprocal of the square of the discharge coefficient) for oscillating flow of water are given in reference 9. At peak oscillation velocities of over 0.5 meter per second, the results show reasonably good agreement with accepted values for continuous flow. In particular, σ is approximately 2.6 for an orifice in a thin plate and 1.5 for length-diameter ratios greater than 1.

The minimum required duct area depends on the maximum expected flow amplitude and the maximum allowable increase in resistance.
A suggested criterion for allowable resistance is

$$R_{nl} < \frac{1}{4} Z'$$

when

$$Q = \frac{\ddot{x}_g A}{\omega_n}$$

where the sinusoidal acceleration $\ddot{x}_g$ is the maximum expected quasi-sinusoidal response of the structure to extraneous disturbance (ringing level).

Using these expressions in equation (B5) gives the minimum required area

$$S = \sqrt{\frac{1.7\ \sigma\rho A\ddot{x}_g}{Z'\omega_n}} \tag{B6}$$

APPENDIX C

EXAMPLE

The general configuration of the vehicle selected as an example is shown in figure 7. Hydrocarbon fuel is stored in the upper tank and liquid oxygen in the lower. Values of pertinent vehicle and propellant-system parameters are presented in table I. All dimensional parameters are given in inch - pound force - second units. Equivalent units in the International System are listed in appendix A. (Since this is an hypothetical example for illustrative purposes only, the actual numbers are of no special significance. Therefore, use of both systems of units in text and and tables would serve no useful purpose.)

The solution of any design problem is subject to certain constraints imposed by the practical aspects of the situation. It is assumed in the present case that the following conditions have been established:

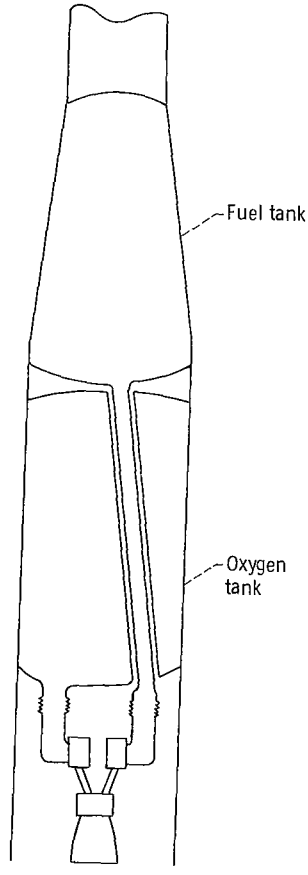

Figure 7. - General configuration of example.

TABLE I. - HYPOTHETICAL VEHICLE PARAMETERS

(a) Fixed parameters

System	Density, ρ, lb-sec^2/in.^{4}	Thrust-chamber partial-resistance coefficient, H, lb-sec/in.^{5}	Suction-line area, S_s, in.^{2}	Suction-line length, l_s, in.^{2}	Sonic speed, a_s, in./sec	Total resistance, $R_p + R_d$, lb-sec/in.^{5}	Total inertance, $L_p + L_d$, lb-sec^2/in.^{5}	Modal velocity ratio of pump, φ_p	Kinematic factor, k	Ratio of mean thrust to mean chamber pressure, S_E, in.^{2}	Thrust-chamber time constant, τ_c, sec
Oxygen	1.06×10^{-4}	0.034	36	30	-------	0.110	9×10^{-4}	1.0	0	285	0.0025
Fuel	.795	.030	22	320	2.8×10^{4}	.165	14.1	1.0	-.78	285	.0025

(b) Time-dependent parameters

Burn time, percent	Modal angular frequency, ω_n, sec^{-1}	Effective modal mass, M_n, lb-sec^2/in.	Modal velocity of liquid center of mass, φ_q		Pump gain, m + 1		Liquid level, h, in.		Suction pressure, P_s, psi		Caviation compliance, C_b, in.^{5}/lb	
			Oxygen	Fuel	Oxygen	Fuel	Oxygen	Fuel	Oxygen	Fuel	Oxygen	Fuel
0	72	2600	1.0	-0.50	1.0	1.0	250	200	61	62	0.04	0.02
60	92	500	↓	-.24	1.3	↓	110	83	45	42	.20	.04
80	104	180		.18	1.8		63	50	43.5	50	.40	.03
95	126	50		.50	3.0		27	23	41.5	61	.75	.021
100	148	25	↓	.58	5.4	↓	15	15	40.5	65	1.50	.019

TABLE II. - PROPELLANT SYSTEM CALCULATIONS

(a) Calculations based on equations (40) and (41)

System	Burn time, percent	Area, $in.^2$	Effective resistance looking into pump, R', $lb\text{-}sec/in.^5$	Effective reactance looking into pump, X', $lb\text{-}sec/in.^5$	Force-feedback scale factor, K	Driving-force term, $\frac{1 - i\frac{X'}{R'}}{1 + i\omega\tau_c}$	Retarding-force term, $\frac{A\lvert Z'\rvert^2}{S_E HR}$	Force-feedback amplitude factor, Ω	Force-feedback phase angle at resonance, θ, deg	In-phase component of force-feedback function, ξ	
										Maximum	Minimum
Oxygen	0	336	0.144	0.059	0.0087	0.90 - i0.57	5.85	4.98	-173.4	0.00015	-0.0431
	60	168	.111	.058	.0163	0.84 - i0.72	3.80	3.04	-166.5	.00067	-.0488
	80	112	.080	.047	.0290	0.79 - i0.79	1.24	.91	-119.4	.00675	-.0198
	95	68	.048	.034	.0526	0.71 - i0.94	.56	.96	-81.2	.0290	-.0212
	100	54	.027	.022	.0705	0.61 - i1.06	.26	1.12	-71.5	.0520	-.0270
Fuel	0	40	0.195	0.096	0.0009	0.88 - i0.65	1.13	0.70	-110.9	0.00021	-0.00043
	60	42	↓	.123	.0036	0.81 - i0.81	1.33	.96	-122.5	.00080	-.00265
	80	37		.139	.0084	0.76 - i0.91	1.27	1.04	-119.0	.00225	-.0065
	95	32		.168	.0215	0.66 - i1.07	1.26	1.22	-119.3	.00671	-.0196
	100	31		.197	.0353	0.55 - i1.00	1.40	1.31	-130.3	.00820	-.0381

(b) Calculations based on equation (42)

System	Burn time, percent	Unmodified susceptance, B_u, $in.^5/lb\text{-}sec$	Force-feedback detuning angle tangent, $\tan\psi$	Force-feedback detuning angle, ψ, deg	Force-feedback phase angle, $\psi + \theta$, deg	In-phase component of force-feedback function, ξ
Oxygen	0	-154	26.4	87.8	-85.6	0.00012
	60	-105	15.3	86.3	-80.2	.00055
	80	-67	7.78	82.7	-36.7	.00273
	95	4.5	.39	21.2	-60.0	.0234
	100	45	-1.23	-50.9	-122.4	-.0267
Fuel	0	-7.7	2.37	67.1	-43.8	0.00018
	60	-2.0	1.18	49.9	-72.6	.00067
	80	-.86	.96	44.0	-75.0	.00163
	95	1.6	.328	18.2	-101.1	-.00480
	100	4.0	-.58	-30.1	-160.4	-.0377

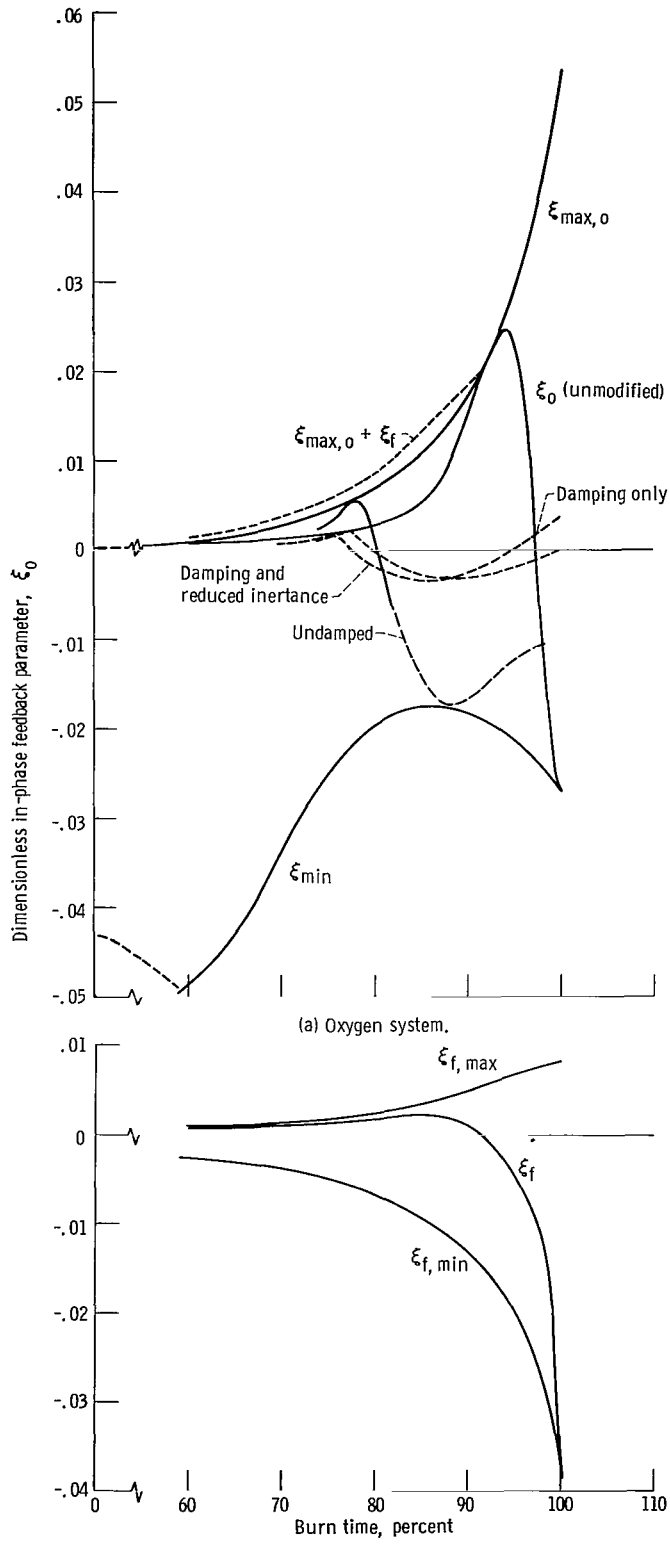

Figure 8. - In-phase thrust feedback.

(1) The accumulator is to have the configuration shown in figure 5(c), using a flexible bellows precharged with nitrogen.

(2) Friction in the duct and bellows is negligible, but damping may be provided, by packing the gas volume with a mesh of fine wire to promote heat transfer (see appendix B).

(3) The structure damping factor is estimated to be 0.015, and a safety factor of two is regarded as necessary; therefore, the maximum allowable value of $\xi_o + \xi_f$ is 0.0075.

Envelopes of maximum and minimum values of the dimensionless in-phase thrust-feedback parameter ξ were determined for both propellant systems by using equations (40) and (41). These calculations are summarized in table II(a). Additional calculations using equation (42) to determine ξ for the unmodified systems are listed in table II(b). Results are plotted as a function of percent burn time in figure 8.

The curve of ξ_o for the unmodified oxygen system in figure 8(a) shows that the oxygen system alone would make the vehicle unstable at the 1.5 percent level from 90 to 96.5 percent burn time. The corresponding curve for the fuel system (fig. 8(b)) shows a maximum ξ_f of 0.002 to 0.0025 at about 85 percent burn time. These results indicate that the oxygen system requires modification; but the fuel system can be let alone since it contributes little to the instability. Therefore, the accumulator for the oxygen system is to be designed to stabilize the vehicle with the fuel system unmodified. In order to provide for consideration of the fuel system in selecting a design point for the oxygen system, a curve showing $\xi_f + \xi_{max,o}$ was plotted on the oxygen-system diagram (fig. 8(a)). This curve shows, for a portion of the flight, the combined effect of the unmodified fuel system plus the maximum possible effect of the oxygen system.

Within the assumed "ground rules", a reasonable procedure would be to design an undamped accumulator to make the maximum system feedback equal to 0.0075 and then calculate the effect of adding damping (and increased compliance) by heat conduction, in the hope of improving the margin.

Circuits representing the specified accumulator types were obtained by combining the elements described in appendix B. The circuit of the undamped accumulator with bellows is shown in figure 9(a) and a simplified equivalent in figure 9(b). With heat-conduction damping, the effective circuit is that shown in figure 9(c).

Examination of figure 8(a) shows that the maximum value of $\xi_o + \xi_f$ will not exceed 0.0075 if the maximum value of ξ_o is made to occur at 78 percent burn time or before. The following conditions at 78 percent burn time were obtained by interpolation from tables I and II for the oxygen system:

$\omega_n = 102.5$ radians/sec $\quad \theta = -124^o$

$P_s = 43.7$ psi $\quad X' = 0.048$ lb-sec/in.^{5}

$B_u = -71$ in.^{5}/lb-sec $\quad R' = 0.083$ lb-sec/in.^{5}

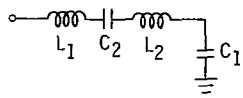

(a) Undamped accumulator, actual circuit.

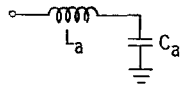

(b) Undamped accumulator, equivalent circuit.

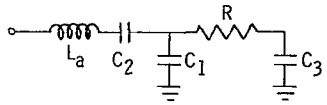

(c) Damped accumulator.

Figure 9. - Circuits representing accumulator with bellows; L_1, duct inertance; L_2, bellows inertance; $L_a = L_1 + L_2$; C_1, adiabatic compliance; C_2, bellows compliance; $C_a = 1/[(1/C_1) + (1/C_2)]$; $C_1 + C_3$, isothermal gas compliance; $RC_3 = \tau_h$ (thermal time constant).

The condition that $\xi = \xi_{max}$ is $\psi = -1/2\ \theta = 62^o$, and the total required susceptance B is

$$B = \frac{X' - R' \tan \psi}{|Z'|^2} = -12 \text{ in.}^5/\text{lb-sec}$$

Therefore, the accumulator susceptance requirement is

$$B_a = B - B_u = 59 \text{ in.}^5/\text{lb-sec}$$

Since B_a must be positive at all times, $\omega_n^2 L_a C_a$ must be less than 1 at cutoff. The bellows stiffness is to be small compared to that of the gas; therefore, the net compliance is roughly proportional to $1/P_s^2$ and at cutoff is not more than 1.17 times its value at 78 percent burn time. To provide a margin, $\omega_n^2 L_a C_a$ is set equal to 0.8 at cutoff. Then at 78 percent burn time,

$$L_a C_a = \frac{0.8}{148^2 \times 1.17} = 0.31 \times 10^{-4} \text{ sec}^2$$

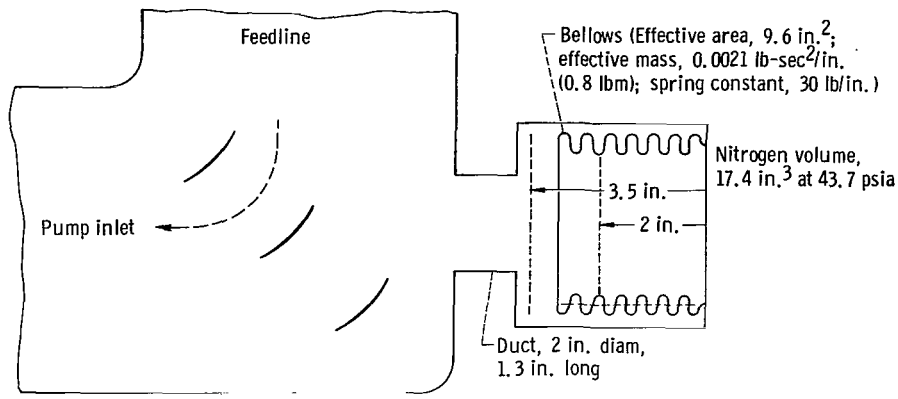

Figure 10. - Accumulator for liquid-oxygen system.

$$B_a = \frac{\omega_n C_a}{1 - \omega_n^2 L_a C_a} = 1.48\ \omega_n C_a = 59 \text{ in.}^5/\text{lb-sec}$$

Therefore, $C_a = 0.39$ in.^{5}/lb and $L_a = 0.8\times10^{-4}$ lb-sec^2/in.^{5}.

A tentative design based on these parameters is shown in figure 10. Since the maximum value of ξ_o was selected as the design point, no further calculations are necessary for the undamped case. It is known that ξ_o falls quickly to negative values after 78 percent burn time and remains negative thereafter because $\omega_n^2 L_a C_a < 1$ at cutoff. The curve of ξ_o as a function of time for the modified system is sketched roughly in figure 8.

To evaluate the effect of damping by heat conduction, the same design was used except that the nitrogen volume was assumed to be packed with fine wire. The equivalent circuit is shown in figure 9(c). The accumulator admittance at 78 percent burn time ($\omega = 102.5$) was calculated by using three values of the time constant τ_h corresponding to $\tau_h\omega_n = 0.5$, 1.0, and 2.0. Values of admittance were found to be, respectively, $15 + i86$, $18 + i75$, and $14 + i65$ inch^5 per pound-second. Note that the susceptance is larger than for the undamped case because of the increase in effective compliance. Calculation of ψ shows that ξ_o is negative (because $\psi + \theta < -90^o$) at 78 percent burn time for all three values of R, indicating that the peak value occurs somewhat earlier where the envelope ξ_{max} is lower. Of more importance is the effect of damping in reducing the peak value of ξ_o by making λ less than 1. Values of λ calculated for the three cases (at 78 percent burn time, which is close enough to make them applicable at the peak) were 0.37, 0.34, and 0.39. Thus, if the design value of τ_h can be realized within a factor of two, the peak value of ξ is less than 40 percent of that of the undamped system. With the damped accumulator the peak value of ξ_o is approximately 0.0017,

occurring at about 75 percent burn time. Because of the increased effective compliance, the damped accumulator frequency is slightly below the modal frequency at cutoff. For this reason, ξ_o rises above zero to 0.0031 at cutoff, as shown in figure 8(a). Reducing the inertance L_a to 0.7×10^{-4} pound-second^2 per inch^5 would make ξ_o very close to zero at cutoff and increase the peak value only slightly to about 0.022 at 77 percent burn time. At this time, ξ_f for the unmodified fuel system is 0.0014, making the maximum total in-phase feedback for the vehicle $\xi_o + \xi_f$ about 0.0036 with the damped accumulator. (The fact that the peaks of ξ_o for the damped system are nearly tangent to the unmodified curve is accidental.)

Additional checkout calculations would be necessary to investigate the effects of variations in the parameters. Modification of the fuel system also would be desirable as a precaution. A very small undamped accumulator with a working volume of only about 2 cubic inches would make ξ_f negative after about 50 percent burn time.

REFERENCES

1. McKenna, K. J.; Walker, J. H.; and Winje, R. A.: Engine-Airframe Coupling in Liquid Rocket Systems. J. Spacecraft Rockets, vol. 2, no. 2, Mar.-Apr. 1965, pp. 254-256.

2. Bikle, F. E.; and Rohrs, J. B.: Dynamic Analysis of Longitudinal Oscillations of SM-68B Stage I (POGO). Rep. CR-64-71, Martin Co., Mar. 1964. (Available from DDC as AD-461795.)

3. Rubin, Sheldon: Longitudinal Instability of Liquid Rockets Due to Propulsion Feedback (POGO). J. Spacecraft Rockets, vol. 3, no. 8, Aug. 1966, pp. 1188-1195.

4. Rose, Robert G.; Simson, Anton K.; and Staley, James A.: A Study of System-Coupled Longitudinal Instabilities in Liquid Rockets. Part I: Analytical Model. Rep. GD/C-DDE65-049, pt. 1, General Dynamics/Convair (AFRPL-TR-65-163, pt. 1, DDC No. AD-471523), Sept. 1965.

5. Rose, Robert G.; Simson, Anton K.; and Staley, James A.: A Study of System-Coupled Longitudinal Instabilities in Liquid Rockets. Part II: Computer Program. Rep. GD/C-DDE65-049, pt. 2, General Dynamics/Convair (AFRPL-TR-65-163, pt. 2, DDC No. AD-471508), Sept. 1965.

6. Lewis, William; and Blade, Robert J.: Analysis of Effect of Compensating-Bellows Device in a Propellant Line as a Means of Suppressing Rocket Pump Inlet Perturbation. NASA TN D-2409, 1964.

7. Mechel, F.; Mertens, P.; and Shilz, W.: Research on Sound Propagation in Sound-Absorbent Ducts with Superimposed Air Stream. Vol. 3. Göttingen Univ. (AMRL-TDR-62-140, DDC No. AD-296984), Dec. 1962.

8. Blade, Robert J.; and Holland, Carl M.: Attenuation of Sinusoidal Disturbances in Nonviscous Liquid Flowing in a Long Line with Distributed Leakage. NASA TN D-3563, 1966.

9. Thurston, George B.; Hargrove, Logan E., Jr.; and Cook, Bill D.: Nonlinear Properties of Circular Orifices. J. Acoust. Soc. Am., vol. 29, no. 9, Sept. 1957, pp. 992-1001.

NASA-Langley, 1969 — 28 E-5055

"The aeronautical and space activities of the United States shall be conducted so as to contribute . . . to the expansion of human knowledge of phenomena in the atmosphere and space. The Administration shall provide for the widest practicable and appropriate dissemination of information concerning its activities and the results thereof."

—NATIONAL AERONAUTICS AND SPACE ACT OF 1958

NASA SCIENTIFIC AND TECHNICAL PUBLICATIONS

TECHNICAL REPORTS: Scientific and technical information considered important, complete, and a lasting contribution to existing knowledge.

TECHNICAL NOTES: Information less broad in scope but nevertheless of importance as a contribution to existing knowledge.

TECHNICAL MEMORANDUMS: Information receiving limited distribution because of preliminary data, security classification, or other reasons.

CONTRACTOR REPORTS: Scientific and technical information generated under a NASA contract or grant and considered an important contribution to existing knowledge.

TECHNICAL TRANSLATIONS: Information published in a foreign language considered to merit NASA distribution in English.

SPECIAL PUBLICATIONS: Information derived from or of value to NASA activities. Publications include conference proceedings, monographs, data compilations, handbooks, sourcebooks, and special bibliographies.

TECHNOLOGY UTILIZATION PUBLICATIONS: Information on technology used by NASA that may be of particular interest in commercial and other non-aerospace applications. Publications include Tech Briefs, Technology Utilization Reports and Notes, and Technology Surveys.

Details on the availability of these publications may be obtained from:

SCIENTIFIC AND TECHNICAL INFORMATION DIVISION

NATIONAL AERONAUTICS AND SPACE ADMINISTRATION

Washington, D.C. 20546